A robust superhydrophobic coating of SER/ ZnO/MWCNTs with high corrosion resistance was prepared by one-step spraying method

F. H. Liang[a], F. F. Mao[a], C. Q. Li[a*], J. F Ou[a], W. Li[a], F. J. Wang[a], A. Amirfazli[b]
[a]*School of Materials Engineering, Jiangsu University of Technology, Changzhou, 213001, P. R. China*
[b]*Department of Mechanical Engineering, York University, Toronto, ON, M3J 1P3, Canada*

Multifunctional integration is the basic feature of artificial superhydrophobic coatings widely used in many fields. This paper presents a simple and economical experimental method to prepare a super hydrophobic coating with super strong corrosion resistance by spraying a mixed solution composed of epoxy resin (EP) as the base, multi-walled carbon nanotubes (MWCNTs), sericite (SER), nano-zinc oxide (ZnO) and octadecyl trimethoxysilane (ODTMS) on an aluminum substrate. Firstly, the superhydrophobic property of the coating prepared in this experiment is better than that of the ordinary coating, and its contact angle reaches 167.3° and rolling angle is as low as 2.7°. Secondly, the superhydrophobic coating can not only maintain the superhydrophobic property in harsh environment (such as: soaking in boiling water for 10 hours, soaking in acid, alkali and salt solution for 7 days, high temperature, burning and strong ultraviolet irradiation, etc.), but also can withstand a variety of mechanical damage without losing the superhydrophobic property (such as: 1000 sandpaper wear cycles, 100 tape stripping cycles and 1000 g grit sustained impact). In addition, the excellent non-wettability of superhydrophobic coating can make it have excellent performance in the field of self-cleaning and anti-fouling. It is worth mentioning that the electrochemical workstation experiment proved that the coating also has good corrosion resistance, and the anti-corrosion efficiency reached 99.924%. This strong superhydrophobic coating has many functions, such as self-cleaning, antifouling and corrosion prevention, and will have good application prospects in many fields in the future.

1. Introduction

Metals and metal alloys, as core engineering materials, play an irreplaceable role in many industrial fields, such as production and manufacturing in traditional industries, parts manufacturing in the machinery industry, and related developments in the agricultural field. However, they are vulnerable to corrosion, resulting in shortened engineering life, huge economic losses and threats to life safety [1,2]. Nowadays, the main way to prevent metal corrosion because of rust is to use the principle of electrochemical workstation to protect [3,4], adding corrosion inhibitor protection [5-7], surface spraying coating protection [8,9] and so on. Among them, coating protection law is an effective method to prevent metal corrosion, simple operation and low cost. Polymer resins (e.g., epoxy and polyurethane) are widely used in coating protection [10]. However, the function of these anti-corrosive coatings is only to separate the metal or some alloy of the metal from the medium containing the corrosive material. After a short time, the corrosive medium can penetrate the coating in direct contact with it, and the metal or metal alloy surface begins to be corroded by the corrosive medium [11,12]. Therefore, we have found a new method to effectively reduce the corrosion rate of the coating, by reducing the contact between the corrosive substance

and the actual use of the coating, greatly improving the service life of the metal or alloy.

The liquid contact Angle of the artificial superhydrophobic composite surface has certain requirements, so does the rolling Angle, which is inspired by the behavior of some natural organisms, such as the shell of a beetle in the desert [13], the drops of water on a lotus leaf in the rain [14,15] and the wings of a butterfly flying in the rain [16]. During the decades of superhydrophobic surface research, its great potential for application in metal corrosion, anti-icing, self-cleaning has brought it remarkable attention in material science [17-26]. A rough surface structure and a lower surface potential energy are two basic characteristics of superhydrophobic coatings [27]. Now the problem is how to better control the microstructure of the superhydrophobic surface, people have come up with many methods, such as template control method, chemical etching method and anodic oxidation method [28-31]. The spraying method of superhydrophobic coating can meet the needs of mass production, and is deeply loved in the field of superhydrophobic coating preparation. Cui et al. [32] prepared an extremely corrosion-resistant superhydrophobic composite coating by spraying and micro-arc oxidation. Lv et al. prepared fluoride-free PS superhydrophobic composite coating by a simpler spraying method [33]. Guo et al. [34] obtained an antibacterial superhydrophobic composite coating by spraying carboxyl polybenzene sulfide (PPS-COOH), fluorosilane-modified zinc oxide (FAS-ZnO) and asphalt (ATP) on iron base.

From another point of view, most of the existing superhydrophobic composite coatings have the defect of poor mechanical durability, this makes the practical application of superhydrophobic composite coating very difficult. The experiments of Xiu et al. [35] prove that after mechanical wear, superhydrophobic composite surfaces with micro - and nano-scale microstructure are more complete than those with only nano-scale microstructure.

Based on the above reasons and considering the harmful materials in destroying the ecological environment at the same time and also harm human health, so need to develop a simple operation, economical and can meet the demand of mass production method, namely in the substrate surface preparation from cleaning, anti-fouling, corrosion prevention and other functions in the integration of strong super hydrophobic coating has important practical significance.

In this experiment, we adopted a simple, convenient and efficient spraying process to prepare SER/zinc oxide/MWCNTs composite superhydrophobic coating on the surface of ordinary aluminum sheets. The prepared coating has excellent non-wetting properties, with contact angles up to 167.3 and rolling angles as low as 2.7. The strong adhesion of EP to the substrate, combined with the high wear resistance of SER powder with zinc oxide and MWCNTs nanoparticles, the superhydrophobic coating showed strong mechanical stability in both circulating tape stripping tests and sandpaper wear cycle tests. It is worth mentioning that the super hydrophobic coating can maintain excellent stability even in boiling water, burning, acidic, alkaline, ultraviolet irradiation and other environments. In addition, the results of dynamic potential polarization curve (Tafel) and electrochemical impedance spectroscopy (EIS) of the superhydrophobic coating were analyzed and demonstrated. Through data analysis, the superhydrophobic composite coating has good chemical corrosion resistance. This experiment successfully prepared a kind of superhydrophobic coating with good anti-corrosion potential for metal corrosion protection.

2. Experimental section

2.1. Materials

Epoxy resin (EP E51), curing reagent (D-230) and octadecyl triethoxysilane (ODTMS) were all supported by McLean (China). NaCl, NaOH, HCl and anhydrous ethanol are all standard liquids and can be used without further operation, purchased from Shenyang Chemical. Zinc oxide nanoparticles (n-ZnO 20nm) were provided by Shandong Yanggu Zhongtian Zinc Industry Co., LTD. Multi-walled carbon nanotubes (CNT-010-0) were purchased from Gaad Chemical. Sericite (SER 600) provided by Shenzhen Haiyang Powder. Aluminum sheets are purchased from local markets for pretreatment before use.

2.2. Preparation of strong anticorrosive superhydrophobic coating

First, use 240 mesh and 800 mesh sandpaper to polish the aluminum side (5*5 cm2) in turn to remove the surface impurities of the aluminum plate. Then clean the aluminum plate with ethanol until there is no dirt, then rinse the ethanol with deionized water, cycle twice, and finally put the cleaned aluminum plate into a vacuum drying oven for drying.

The following are the experimental steps for the preparation of strong corrosion resistant superhydrophobic coating in this experiment. First, 3.6g EP was added to 25 mL of ethyl acetate (EA); Then, 3 g n-ZnO, 1gSER and a certain amount of MWCNTs were added to the solution from 0.1g to 0.5g at 0.1g intervals, and drip-supplemented with 200 μL ODTMS, the mixing solution was then stirred for 2 h; after stirring, sonicated for 30 min, prevent polyization of micro and nanoparticles in mixed solution; continue stirring for 3 hours, Ensure that the micro-nanoparticles are evenly dispersed; finally, D-230 was added and stirred. Finally, by spraying the obtained mixed solution on the base aluminum plate, the super hydrophobic composite coating of SER&ZnO &MWCNTs with wear resistance and corrosion resistance can be prepared. FIG. 1 shows the preparation of the composite coating.
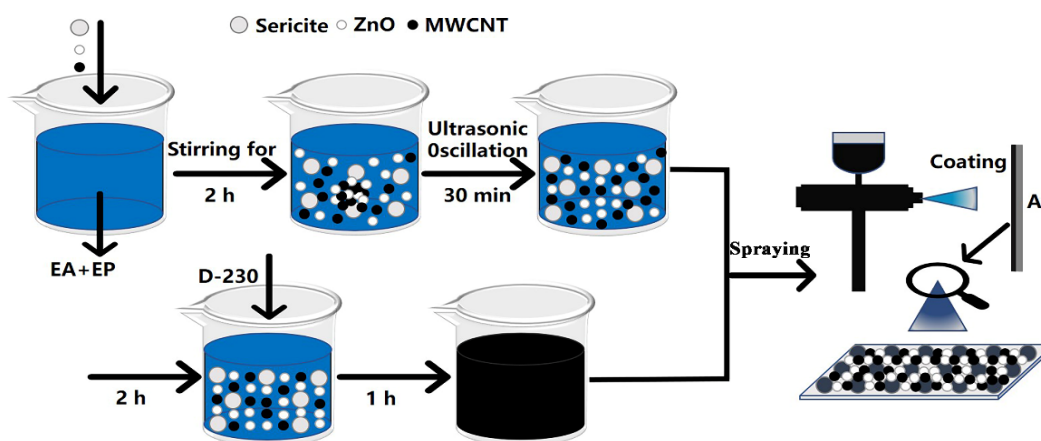

Fig. 1. Diagram of preparation process of superhydrophobic coating

2.3 Surface characterization

The surface composition of the coating was analyzed using FTIR spectroscopy (FTIR, Jasco). The surface morphology of these coatings was observed by scanning electron microscope (SEM, FEG 400) at an accelerated voltage of 15 kV. The wettability of the coating surface of the sample was tested using a contact angle measuring instrument (Fed-A1, Kezon) with a drop volume of 10 μL and measured at 5 different locations. The final result was obtained by averaging the five sets of data. Tilt the surface of the coated sample slightly, and the water droplets drop from about 1cm above it. If the water droplets can roll off, the sample is then tilted at a reduced Angle, and the water continues to drip until it no longer rolls over the composite coating surface, record the angle at this time as the rolling angle, repeat the above steps five times, and take the average of the five times as the final rolling angle.

2.4. Mechanical stability testing

Common tests for coating stability testing include sandpaper wear test, tape test, gravel impact test and adhesion test.

Sandpaper wear test: wear testing machine is used to test the wear resistance of the sample. Tape stripping test: First, the tape is tightly fitted to the super hydrophobic coating, and then the tape is quickly stripped.

Gravel impact test: tilt the sample to 45 to release sand from above the sample to impact the sample. For the above tests, test and record the contact Angle and rolling Angle of the sample every 5 cycles.

2.5. Physical / Chemical durability test

Acid-alkali salt test: Place a coating sample in a strong acid solution, a strong alkali solution and a 3.5wt%NaCl solution, take it every 24h, clean it and put it in the oven to dry. Finally, the contact Angle and rolling Angle of the sample need to be measured and recorded again.

Burning, high temperature and ultraviolet aging test: the sample is placed on the flame of an alcohol lamp and burned for a certain period of time. After burning, the alcohol lamp is extinguished. After cooling, the contact angle of the sample is measured and its self-cleaning performance is tested.The prepared sample is placed in a Muffle furnace and held at 50 ° C from 100°C to 300°C for 2 hours. After the sample furnace cools, the contact angle and rolling angle are measured and recorded again. The sample was irradiated under an ultraviolet lamp, the lamp was 15-20 cm away from the coating sample, and the relevant parameters were adjusted (the power was 2.2kw, the nominal ultraviolet wavelength was 313 nm) for ultraviolet irradiation. Samples were taken every 12 hours, and after alternating cleaning and drying with ethanol and deionized water, the contact Angle and rolling Angle of the sample need to be measured and recorded again.

2.6. Self-cleaning and anti-pollution test

The red dye is poured on the surface of the ordinary coating and the superhydrophobic composite coating respectively. Drip water about 1 cm above the coating and observe the pigment taken away when the water drops and rolls. By dipping the superhydrophobic coating into methylene-blue solution, and then remove the coating two hours later and see if any solution sticks to the coating; The sample was tilted at an angle, about 1 cm above it, and several common liquids (including milk, milk tea, cola, dye, mud water and soy sauce) were continuously dropped. It was observed whether several liquids could roll off the surface of the superhydrophobic coating and whether rolling marks would be left after rolling.

2.7. Electrochemical testing

The sample was placed in 3.5 weight.% sodium chloride solution and the electrochemical impedance spectroscopy (EIS) and dynamic potential polarization curve (Tafel) of the coating were measured using Gamry instrument. The electrochemical impedance spectra were collected from the electrochemical impedance spectra curves. The potential polarization curve was scanned at 1 mV/s.

3. Results and discussion

3.1. Wettability analysis

There are two important indicators to evaluate whether the coating is super hydrophobic coating:First, the surface of the coating needs to reach a certain roughness; Second, the surface energy required for the coating is lower[36,37]. In this paper, the surface structure of the coating was constructed using SER, ZnO and MWCNTs, and the effects of different MWCNTs contents on hydrophobicity were investigated. FIG. 2a shows the results of the various tests for the coating. With the increase of MWCNTs content, the contact angle also increased gradually. When MWCNTs achieved the best superhydrophobic effect in the coating, the contact angle reached 167.3, while the rolling angle was only 2.7. Subsequently, when the MWCNTs content was excessive, the contact Angle decreased slightly, but the rolling Angle increased. The analysis in Figure 3 confirms that the coating hydrophobicity increases significantly as (ODTMS) improves the graft coating as a low surface energy substance. Of course, with the increase of MWCNTs content, the coating structure increased roughness and became denser. When the optimal surface roughness was reached, the content of MWCNTs continued to increase and MWCNTs began to accumulate, but the roughness decreased slightly.

In addition, the wettability of different liquids on the surface of the superhydrophobic composite coating is also discussed. Seven different liquids (including milk, milk tea, cola, pigment, soy sauce, acid and alkali) were added to the surface of the sample, and the contact

angles of the different liquids were measured and recorded. Figure 2b shows the test results. All droplets are spherical on the surface of the sample, and each contact Angle is greater than 150. Through observation, it can be found that among the seven liquids, soy sauce and pigment have the smallest contact angle, while several transparent liquids cola, acid and alkali have the largest contact angle. The main reason is that it is harder for dense droplets to maintain sphericity than smaller ones at the same volume.
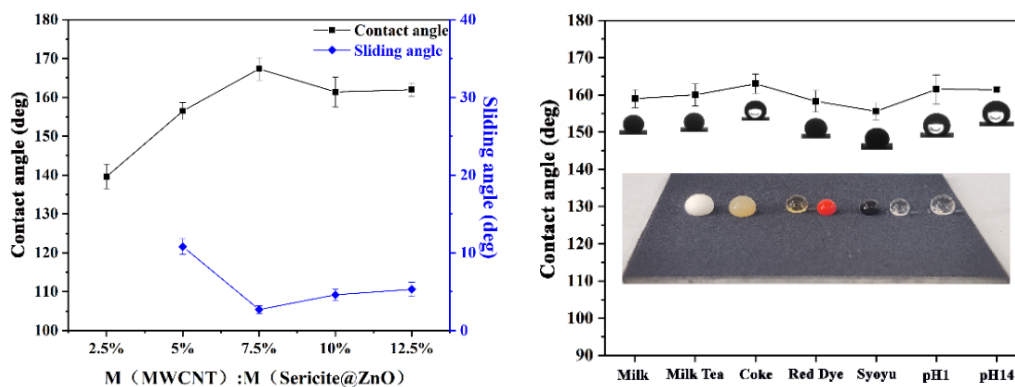

Fig. 2. (a) Effect of MWCNTs content on hydrophobicity of coatings; (b) Hydrophobicity of droplets with different surface tension on coating surface

3.2. Surface morphology and chemical characterization

The microstructure and composition of the composite coating were analyzed by scanning electron microscopy and FTIR spectroscopy. As shown in Figure 3, many micron-scale bumps and nanoscale papillae appear on the obtained dense superhydrophobic coating due to the aggregation of micro-nanoparticles.
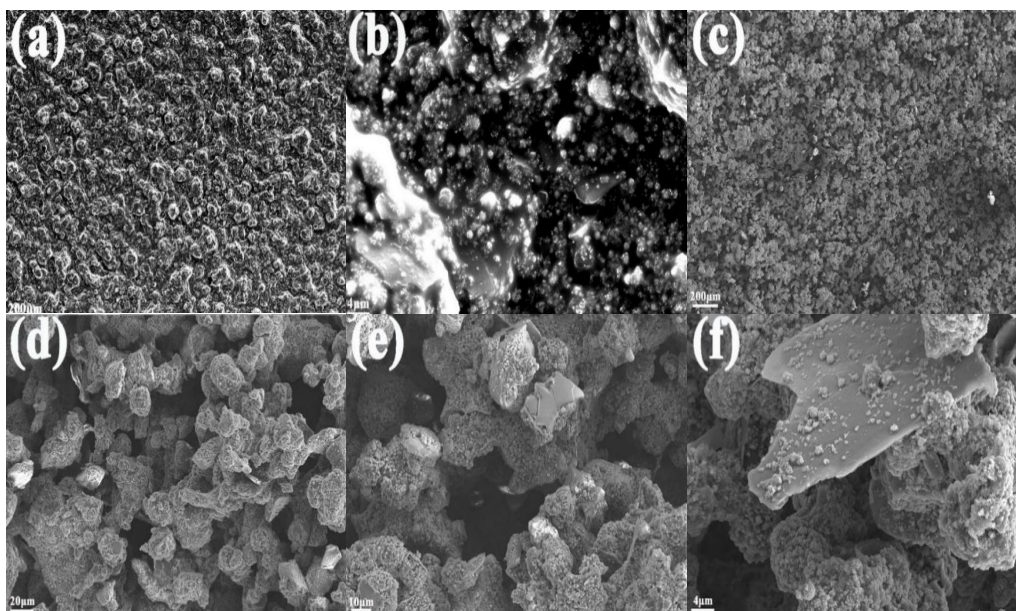

Fig. 3. (a-b)SEM of coatings with 2.5% MWCNTs; (
c-f) SEM diagram of coating with 7.5% MWCNTs content.

Air is present in the space between these nanoscale papillae, and when the sample is eroded by the corrosive solution, this air forms a dense layer to suppress the corrosive solution.

According to the display in Figure 3 (a-b), the content of MWCNTs in the coating is 2.5%, making the surface presents a certain graded rough structure of micro and nano particles. However, these micron-scale bumps and nanoscale papillae are almost entirely covered by EP, and the surface energy difference between the epoxy resin and the micro-nano structure is huge, so the coating is not super hydrophobic. As can be observed in Figure 3 (c-f), the micro-nano graded rough structure of the composite coating surface becomes more significant as the MWCNTs content increases. Furthermore, micron-scale bumps and nanoscale mastoids begin to penetrate the blockade of the epoxy resin. This makes the prepared composite coating not only have excellent rough micro-nano structure, but also have low surface potential energy and excellent superhydrophobic properties.

The FTIR of sericite, ZnO, MWCNTs and their modified particles is shown in Figure 4. According to spectral line b in the figure, the asymmetric stretching vibration of -OH occurs at the wave number of 3626 cm^{-1}, while its symmetric stretching vibration occurs near the wave number of 3382 cm^{-1}. Similarly, the bending vibration of -OH can be clearly seen at wave number 1625cm^{-1}. It is not difficult to conclude that there are hydroxyl groups in the surface structure of the coating and water molecules in the inner space of SER.[38-40]. According to the analysis of b and d in Figure, the vibration peak generated by ODTMS -COOH is near the wave number of 1456cm^{-1}[41]. In spectral line a, the symmetric contraction vibration peak of Si-O-Si is near the wave number 976cm^{-1} [42,43]. The Si-O vibration peaks of silane appear near 752 cm^{-1} and 694 cm^{-1}. In line d, the peak of wave number near 3382 cm^{-1} indicates the stretching and bending vibration absorption peak of hydroxyl group, indicating that many water molecules are adsorbed on the surface of nanometer zinc oxide, and finally the adsorbed hydroxyl group is formed [44-45]. In addition, it should be noted that the peaks of modified SER and ZnO represent -CH2 asymmetric stretching at 2921 cm^{-1}, while symmetric vibration occurs at 2851 cm^{-1} [38]. This also indicates that octadecyl and trimethoxysilane are introduced into the SER and ZnO networks.In the Figure, spectral lines e and f are MWCNTs and modified MWCNTs, and there is no obvious change in the two spectral lines, because the C=C covalent bond composed of carbon nanotubes is the most stable chemical bond in nature. No chemical reaction occurs between MWCNTs and the modifier ODTMS at normal temperature and neutral conditions, so no new functional groups are generated.
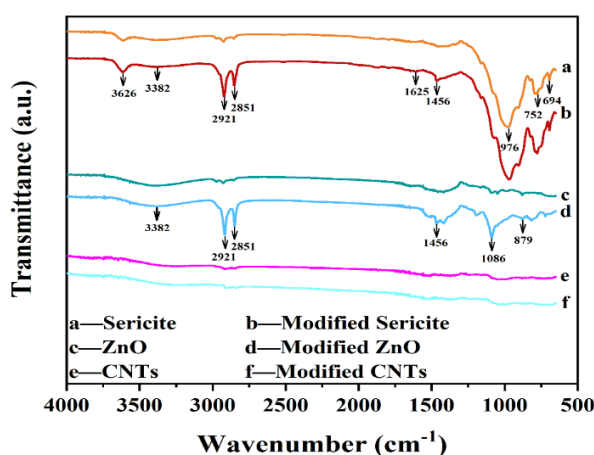

Fig. 4. Infrared spectra of different micro and nano particles.

3.3. Mechanical stability

The main problem facing the application of superhydrophobic coatings is how to enhance their durability, which has a huge impact on the application range. For many of the coatings that have been developed, the porous microstructure of the coating surface is so fragile that even slight friction or direct pressure can destroy the structure[46,47].In this study, the mechanical stability of superhydrophobic composite coating was evaluated through a series of tests, such as sandpaper wear test, tape stripping, sand impact. The system recorded the wettability changes of the sample

after 1400 sandpaper wear cycles and 100 strip stripping cycles, as well as the surface topography changes of the sample after wear cycles, as shown in Fig. 5.The results of FIG. 5c show that the contact Angle of the coating decreases significantly after being worn by sandpaper, and the rolling Angle increases accordingly. When the superhydrophobic coating experienced 1000 sandwear cycles, the contact angle decreased to 151.5, while the rolling angle increased to 21.6. Nevertheless, the coating still maintains a good superhydrophobicity. When the wear period is increased to 1400 times, the contact Angle further decreases to 140.3°, and the rolling Angle gradually increases to 36.6°. The coating loses superhydrophobicity, but still has good hydrophobicity. After 1400 wear cycles of the coating, the comparison between FIG. 5e and FIG. 5f shows that the surface of the composite coating becomes uniform and smooth, because its micro and nano structure is destroyed. It is extremely challenging to maintain superhydrophobic properties of the coating by relying solely on the low surface potential material of the coating surface. Abrasion cycle test of sandpaper shows that the composite coating has good wear resistance[48].
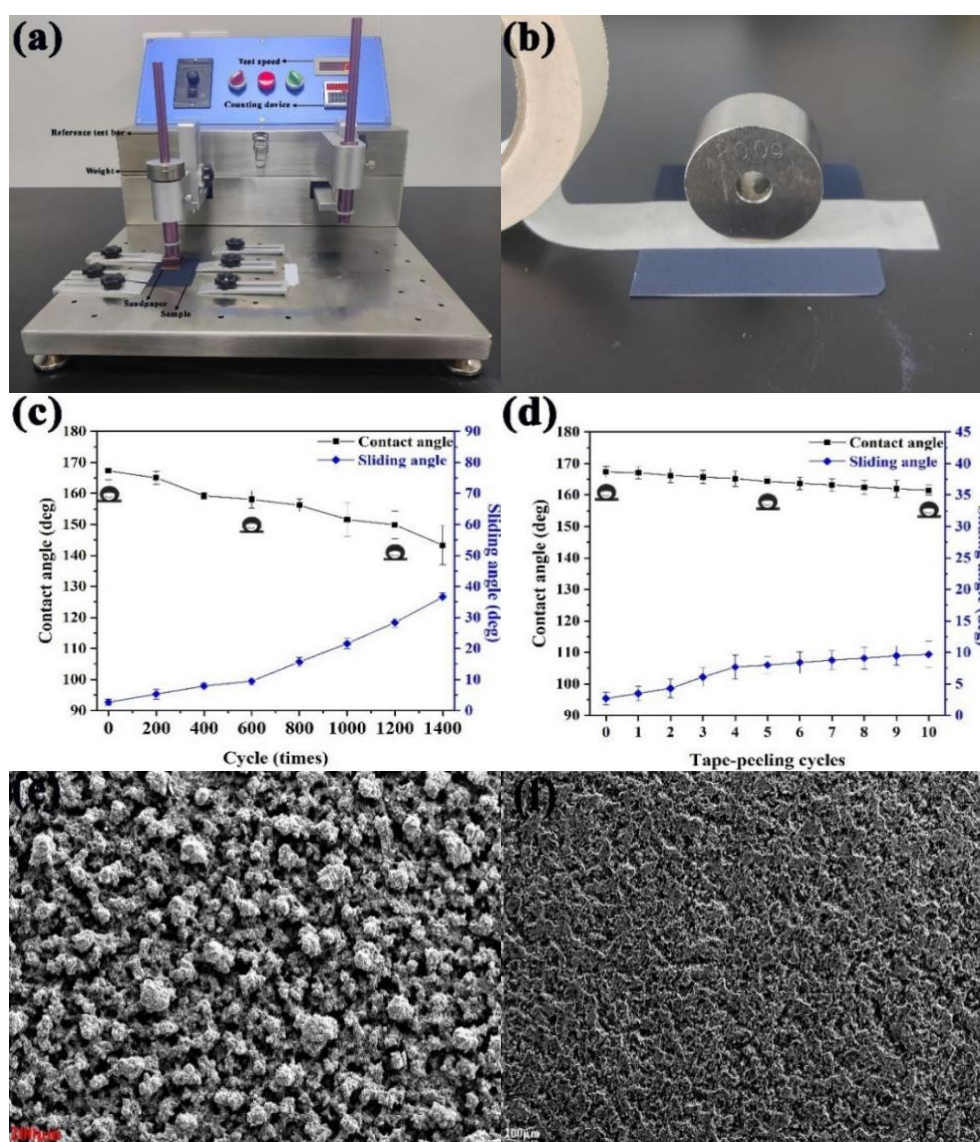

Fig. 5. (a)Schematic diagram of sandpaper wear ; (b)Tape stripping diagram; (c)Relationship between wear frequency and wettability of coating; (d)Coating wettability and stripping times; (e)The SEM images of the initial appearance; (f)The SEM images of the sample after the wear cycle.

Fig. 5b is the schematic diagram of the tape stripping experiment, and Fig. 5d shows the surface wettability changes of the superhydrophobic coating under different cycle conditions in the experiment. As can be seen from Figure 5d, tape stripping has little effect on the superhydrophobic coating. After 100 tape stripping cycles, the contact Angle of the composite coating decreases again to 160.5°, and the rolling Angle increases to 9.7°. These studies and tests show that the superhydrophobic composite coating has excellent durability.

In addition, in order to test whether the mechanical properties of the composite coating are stable, we added a sand impact test. The continuous impact of gravel can destroy the integrity of the coated surface. The results of FIG. 6b show that the continuous impact of gravel will continuously reduce the contact Angle of the coating, and its rolling Angle will continuously increase. The contact Angle of the composite coating decreased to 152.5 ° and the rolling Angle increased to 9.6 ° due to the destruction of the surface structure. The results of the experiment also directly prove that the prepared composite coating has good mechanical stability and can withstand the impact of wind sand in harsh environment [49,50].
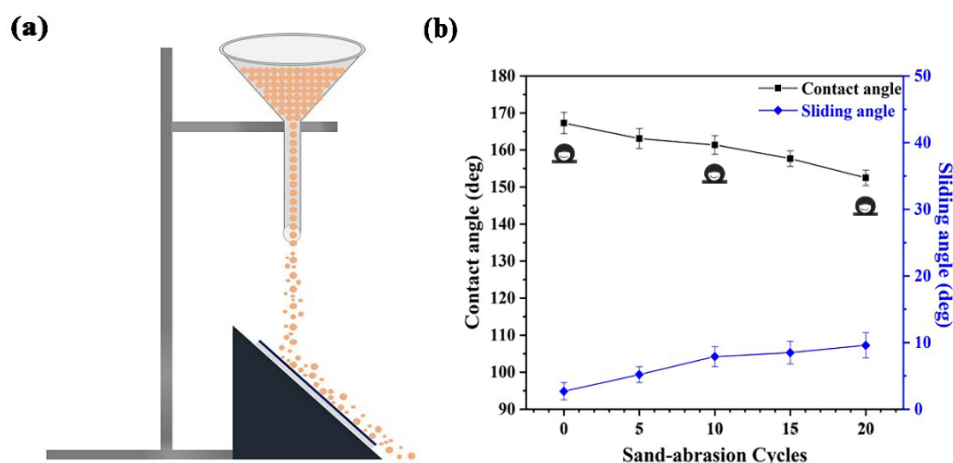

Fig. 6. (a) Sand impact test. Gravel impact model; (b) Relationship between the number of impact cycles of gravel and the wettability of coating.

As we all know, in order to be widely used in practical situations, the super hydrophobic composite coating must have strong adhesion. According to the tape stripping test of international standard ISO2409-2013, as shown in Figure 7c, the cutting edge of the sample is very smooth and the mesh is complete. Compared with the data in Table 1, the binding ability between the superhydrophobic composite coating and the metal substrate is the best. In addition, it can be seen from Figure 7d that even if the superhydrophobic coating is cut in an orderly manner, the droplet can still continue to roll on the surface, indicating that the composite coating still has certain superhydrophobic properties.
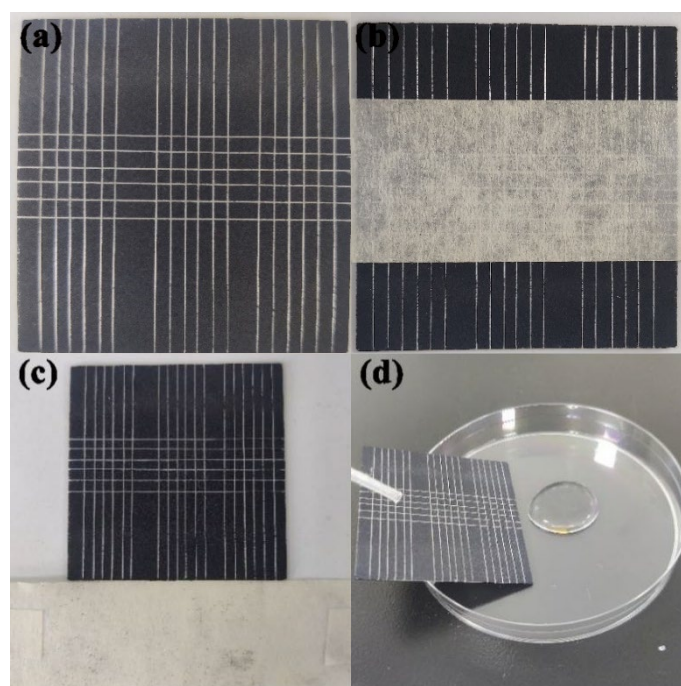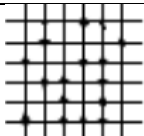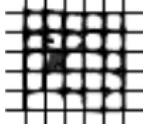
Fig. 7. (a)Cross pattern of superhydrophobic coating surface construction; (b) After tearing it off, a very small amount of powder was placed on the tape ;(c) Cross surface dripping diagram.

Table 1. Classification of experimental results (international standard).

Classification	Illustrate	The appearance of the surface of the cut zone where the detachment occurred (Example)
0	The place where the specimen was cut is intact, and none of the meshes have fallen off	—
1	There is very little coating peeling off where the specimen is cut, but the area of coating peeling off is not more than 5%.	
2	The area where the specimen is cut has more coating peeling than the previous level, and the area of coating peeling off is between 5% and 15%.	

To sum up: superhydrophobic coating has excellent mechanical stability. The main reasons are as follows: firstly, the superhydrophobic composite surface structure based on the combination of microns and nanometers has better wear resistance than a single surface with only nanoscale structure. Secondly, the selected micro and nano particles themselves have better wear resistance. Alternatively, the higher proportion of superhydrophobic coated high epoxy resin used in this study whether it can combine various materials and improve the surface strength of the composite coating [51]. Finally, because carbon nanotubes (CNTs) have an excellent tensile strength and Young's modulus, they are used as nanocomposite packing in many enhanced thermosetting or thermoplastic polymers[52,53].

3.4. Physical/Chemical stability

The durability of superhydrophobic coating is the main reason that it cannot be applied in large quantities in real life [54-56]. For this purpose, the stability of the samples under several harsh environments (including: acid, alkali, salt, boiling water, burning, high temperature and ultraviolet aging) was tested. As shown in Figure 8(a-d), they are respectively strong acid, strong base, 3.5wt.% NaCl solution and boiling water. As shown in Figure 8a, with the increase of soaking time of the sample in a strong acid solution, the coating contact Angle will gradually decrease, but the rolling Angle will continue to increase. After soaking for 24 h, the coating contact Angle will decrease to 165.1° and the rolling Angle will increase to 3.5°. At this time, the sample still has good superhydrophobicity. When the soaking time was extended to 7 days, the contact Angle was further reduced to 154.1°, and the rolling Angle was further increased to 10.9°. The sample still maintained good superhydrophobicity, indicating that the sample had long-term stability in the strong acid solution. It can be seen from Figure 8b that the strong alkali solution has almost no effect on the wettability of the coating. After soaking for 24 h, the contact Angle only decreased slightly, at this time the contact Angle was 166.3°, and the rolling Angle was increased to 3.2°. The sample has excellent superhydrophobicity. When the soaking time was extended to 7 days, the contact Angle was further reduced to 156.2°, and the rolling Angle was gradually increased to 9.7°, indicating that the sample had long-term stability in the strong alkali solution. Figure 8c shows that even after soaking in 3.5 wt.%NaCl solution for more than 7 days, the contact Angle of the coating is still greater than 150°, while the rolling Angle reaches 15°. Figure 8d shows that with the increase of soaking time in boiling water, boiling water has little effect on the coating, and the contact Angle and rolling Angle are almost unchanged. After soaking the sample in boiling water for 2h, the change of contact Angle was 165.7° and the change of rolling Angle was 3.7°, indicating that the sample had good non-wettability. However, after soaking in boiling water for 10 h, the rolling Angle is still less than 10°, and the contact Angle is greater than 150°, indicating that the sample can still maintain good superhydrophobicity after long-term soaking in boiling water. The reason why the wettability of the sample did not change significantly during the initial soaking is that when the composite coating is immersed in the solution, the micro-nano structure of the coating surface can trap the air to form a gas film, which can inhibit the corrosion of the solution on the coating in a short time.
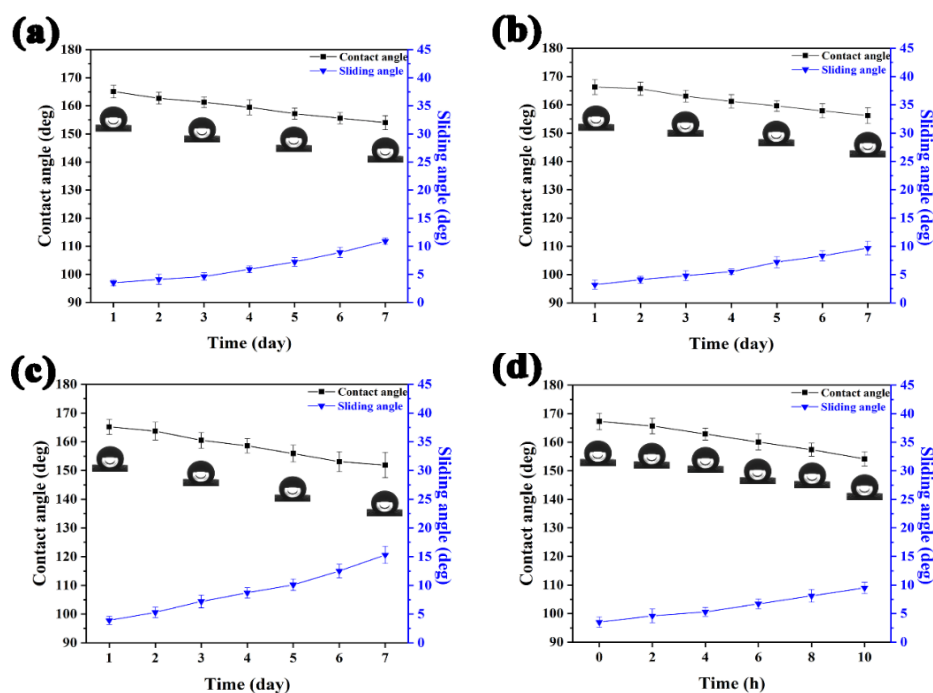

Fig. 8. Durability testing of composite coatings. (a)Strong acid; (b) Strong base;
(c) 3.5 wt.% NaCl solution ; (d)Boiling water.

Burn the sample with an alcohol lamp, as shown in Figure 9a. By comparing Figure 9b and Figure 9c, it can be found that after a period of burning, the surface has left obvious burning traces. After combustion, the contact Angle has a great change from 167.3° to 154.9°, but its super hydrophobic properties still exist. This is also proved by the drip test, as shown in Figure 9(e-f), where the drops quickly fall off the surface of the sample, leaving almost no trace. The self-cleaning test also proves that the sample after burning still has good superhydrophobic property. The burned sample is tilted slightly, and a layer of red pigment is scattered over the burning area. Water droplets are slowly and continuously added to the surface of the sample, and the red pigment is also removed from the surface. As shown in Figure 9 (g-h), the red pigment on the surface of the coating is cleaned after several consecutive drops of water. The test results show that the coating can maintain stable superhydrophobic properties after being burned.
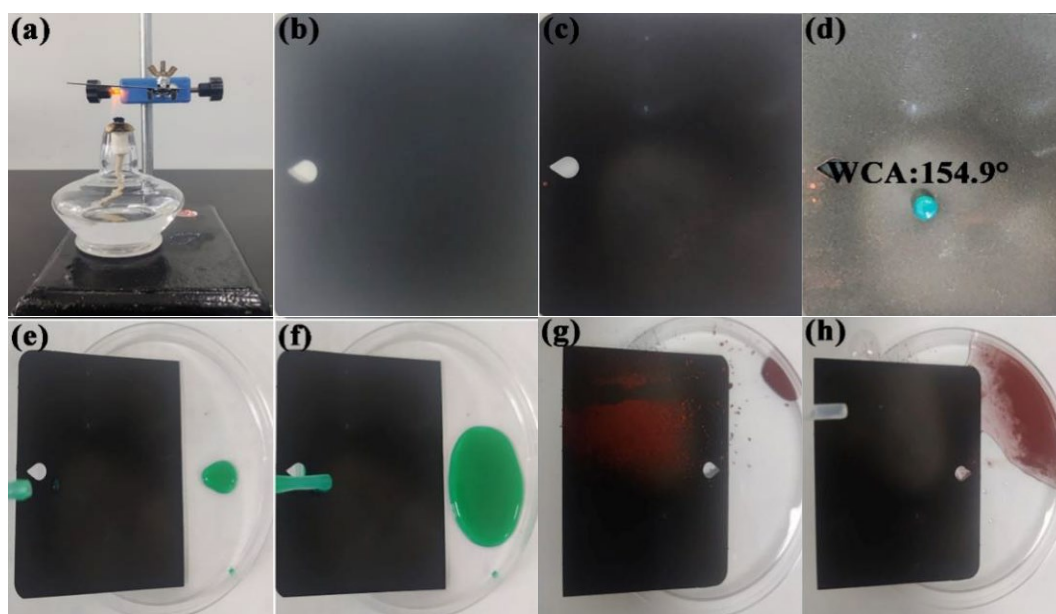

Fig. 9. Burning experiment. (a)Diagram of alcohol lamp burning; (b).The original sample; (c) burning pattern; (d) Contact angle;(e-f) Drip test; (g-h) Self-cleaning.

As shown in Figure 10a, the wettability changes of the composite coating at different temperatures. On the whole, the contact angle changed little, increased or decreased slightly, and the superhydrophobic coating showed excellent high temperature resistance.As can be observed from Figure Figure 10b, the superhydrophobic coating underwent UV irradiation in different time periods, and its wetting state was changed. Among them, the contact Angle of the coating is still greater than 160°, which has good waterproof performance. There are two main reasons: one is that the extinction performance of inorganic filler depends on the different orientation of mineral crystals, thus determining its ability to absorb and reflect ultraviolet light, and sericite is a monocline crystal, has a large refractive index of ultraviolet light. Second, the tightly stacked sericite sheets reflect the incident light layer by layer, which can reduce the light penetration. In short, the superhydrophobic coating with strong durability that has been prepared in this experiment can face a variety of harsh environmental conditions.
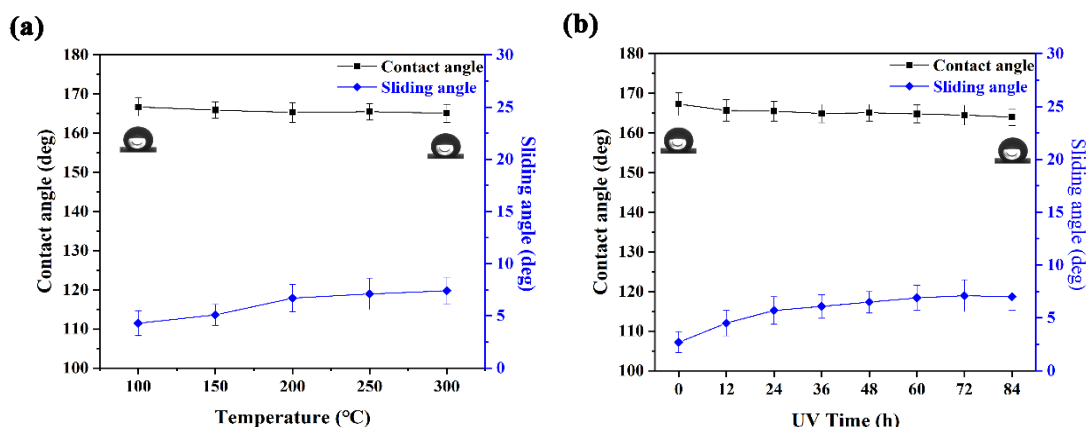
Fig. 10(a) High temperature test; (b) Ultraviolet aging test.

3.5. Self-cleaning and anti-fouling

In practical applications, superhydrophobic composite coatings are usually applied to metal surfaces, which bear the brunt of various types of erosion. Figure 11a shows the self-cleaning diagram of the composite coating. The self-cleaning diagram of the common coating contaminated by red dye is shown in Figure 11 (b1-b3). The self-cleaning diagram of the red dye contaminated superhydrophobic composite coating is shown in Figure 11 (c1-c3). According to Figure 11 (b1-b3), water droplets slowly descend from above the ordinary coating. When the water drops encounter the red paint along the surface, it will continue to slide down, but it is difficult for a single drop of water to slide from the surface of the sample, requiring more water droplets to gather together to complete the process of detachment from the surface.The observation at Figure 11 (c1-c3) shows that when water droplets fall on the super waterproof coating, they do not stay on the surface and instead bounce and roll. These rolling droplets will leave the coating with some iron oxide red paint, leaving a clear rolling path. With the increase of water droplets, the water droplets take red dye with them. The experimental results show that the self-cleaning performance of the composite coating is good.
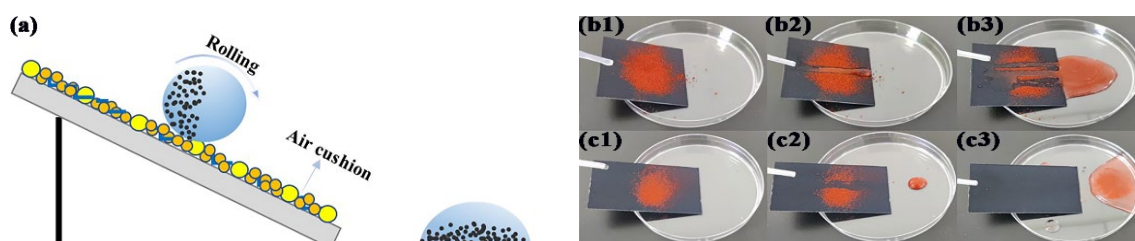

Fig. 11. (a) Schematic diagram of self-cleaning; (b1-b3)Common coating;
(c1-c3) Superhydrophobic coating.

Figure 12 shows the resistance of the superhydrophobic coating to some common droplets (including milk, milk tea, cola, muddy water, soy sauce, dye, etc.). The results showed that drops of milk, milk tea, cola, mud and dye fell on the surface of the sample and quickly rolled off, leaving the surface in the same state as the original. This suggests that the superhydrophobic coating has a strong resistance to these liquids. When the soy sauce falls on the surface of the sample, as shown in Figure 12 (e1, e2), marks are left on the surface of the sample, indicating that the superhydrophobic composite coating is less resistant to soy sauce contamination than the previous liquid. FIG. 12 (g1-g4) shows the erosion process of methylene blue solution protected by the coating. After the superhydrophobic coating is soaked in methylene blue solution, the surface of the coating is completely clean without any traces of contamination. This shows that the

composite coating has superior anti-fouling properties because the liquid cannot penetrate into the microtissue bubbles on the surface, which prevents the coating from being wetted and contaminated, thus exhibiting excellent non-wetting properties[57].
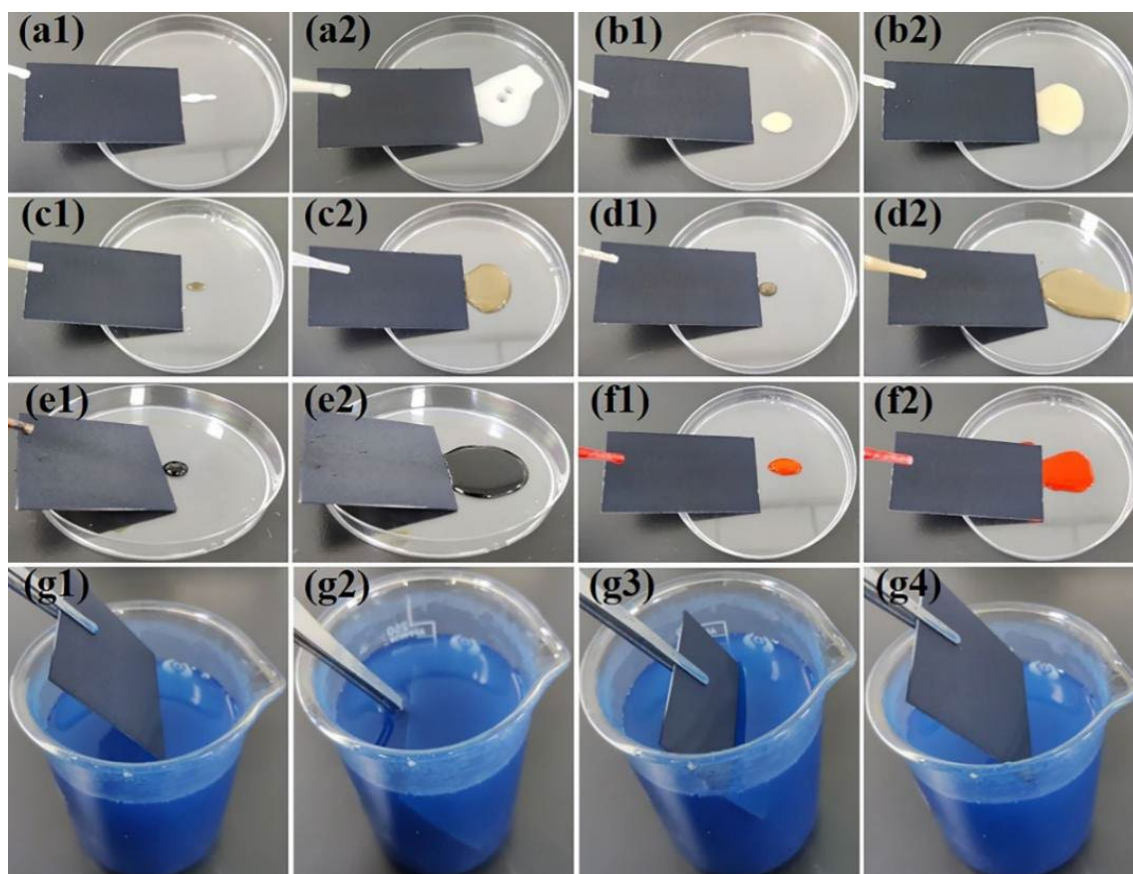

Fig. 12. Resistance of samples to several common liquids: (a1, a2)milk, (b1, b2) milk tea, (c1, c2)cola, (d1, d2)muddy water, (e1, e2)soy sauce, (f1, f2)dye; (g1-g4)Sample antifouling process.

3.6. Electrochemical test
3.6.1. Potentiodynamic polarization curve

The potentiodynamic polarization curves of the initial aluminum sheet, the aluminum sheet sprayed with composite coating and the aluminum sheet soaked in NaCl solution for 24 h, 72 h, 120 h and 168 h are shown in Figure 13. When tested, the potential of the composite coating (Ecorr) shifted in A positive direction by about 1.1 V, while the current (Icorr) dropped by four orders of magnitude from $1.23*10^{-5}$ A • cm^{-2} to $9.320*10^{-9}$ A • cm^{-2}. After 24, 72, 120 and 168 hours, the corrosion current of the coating has a certain decline. When the sample is just immersed, the Icorr changes little, mainly because the air layer on the surface of the composite coating is stable, which can effectively prevent the direct contact of the corrosive medium, and can better protect the super hydrophobic composite coating. Even if the immersion time is extended to 120 hours, the corrosion current (Icorr) of the composite coating is still higher than the current of the initial blank aluminum sheet. When the soaking time is further extended to 168 hours, the corrosion current of the composite coating is not much different from that of the original aluminum plate. The experimental results show that the superhydrophobic composite has good anti-corrosion properties and can effectively play its anti-corrosion role for a long time.
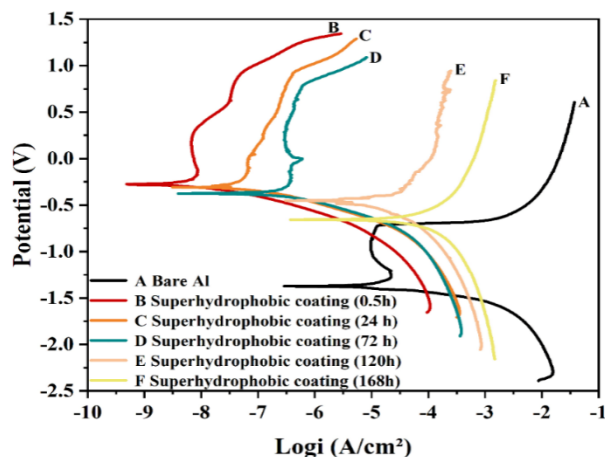
Fig. 13. Potentiodynamic polarization curve of samples soaked in 3.5wt.% NaCl.

In this experiment, Tafel extrapolation method was used to determine the relationship between corrosion potential and corrosion current in the dynamic potential polarization curve, and the anti-corrosion efficiency of the superhydrophobic composite coating was calculated by the formula. (1) [58,59]

$$n_p(\%) = \frac{I_{corr}^0 - I_{corr}^0}{I_{corr}^0} \times 100 \tag{1}$$

Among them, the corrosion current density of superhydrophobic coating samples at different soaking times is 99.992% and 96.88% respectively, it is proved that the composite coating has good corrosion resistance and can maintain high corrosion resistance even after soaking for 72 hours.

Table 2. Fitting results and corrosion inhibition rate of Tafel spectra shown in Fig. 10.

Samples	E_{corr} (V)	I_{corr} (A·cm^{-2})	n_p (%)
Al	-1.370	1.23×10^{-5}	—
Composite coating	-0.278	9.320×10^{-9}	99.92
Immersion for 24 hours	-0.310	3.590×10^{-8}	99.71
Immersion for 72 hours	-0.376	3.84×10^{-7}	96.88
Immersion for 120 hours	-0.452	3.4×10^{-6}	72.36
Immersion for 168 hours	-0.658	9.74×10^{-6}	20.81

3.6.2. Electrochemical impedance spectroscopy

The purpose of EIS analysis is to investigate the properties of superhydrophobic composite coatings and explain the mechanism of corrosion protection. EIS fitting spectra of aluminum sheet and corresponding superhydrophobic coating samples are shown in Figure 14. Figure 14a shows the Nyquist AC impedance profiles of the different samples, where the semicircle arc represents the capacitative loop in the figure. The formation of the capacitor circuit is caused by double layer capacitance transfer. It should be noted that the diameter of the capacitor arc is related to corrosion resistance, and the larger the capacitor arc, the better the corrosion resistance [60]. The polished aluminum substrate is oxidized in the environment, forming a less stable oxide film. However, due to the presence of chloride ions in the solution, the membrane on its surface is destroyed, and the corrosive solution can reach the substrate surface directly. Chloride ions are enriched at the interface of coating/substrate, causing corrosion reactions in the substrate and destroying the combination of coating and substrate, thus, corrosive products will

appear on the base aluminum [61]. As can be observed from Figure 14a, the capacitor arc diameter of the superhydrophobic coating significantly exceeds the capacitor arc diameter of the aluminum sheet. The results also prove that the superhydrophobic composite coating has good corrosion resistance and can improve the service life of aluminum plate. When the sample is immersed in NaCl solution, the micro and nanostructures on the composite coating can store air, which creates reflections. Indeed, the surface area of direct contact with the superhydrophobic coating is reduced by the presence of an air layer. This structure helps to slow down the corrosion process, providing an additional protective layer. After the soaking time is extended to 120 h, the capacitance arc diameter decreases sharply, indicating that the protection ability of the superhydrophobic coating on the aluminum sheet declines sharply, but it is still much greater than the aluminum sheet itself, it is also proved that the superhydrophobic composite coating has good anti-corrosion properties. After soaking for 168 h, the diameter of capacitor arc is smaller than that of aluminum sheet. The longer the sample is soaked, the capacitance arc diameter of the composite coating decreases gradually, indicating that the corrosive medium has contacted the base aluminum plate. This also means that the corrosion resistance of the superhydrophobic composite coating is gradually being destroyed [62,63].

Generally, changes in the low-frequency impedance modulus will affect the corrosion resistance [64]. According to the display of Figure Figure 14c, after soaking the sample of the superhydrophobic coating for 0.5 hours, the low-frequency impedance modulus far exceeded the untreated raw aluminum film. This is because at the beginning of immersion, the superhydrophobic coating remains intact, and the corrosive substance and the base aluminum have not yet come into contact, so the superhydrophobic coating shows excellent corrosion resistance.The longer the sample is soaked, the superhydrophobic composite coating is gradually permeated by corrosive medium, and the low-frequency impedance modulus decreases. When the corrosive medium permeates completely, the composite coating completely loses its function. This process reveals the evolution of superhydrophobic coatings in terms of anti-corrosion properties.
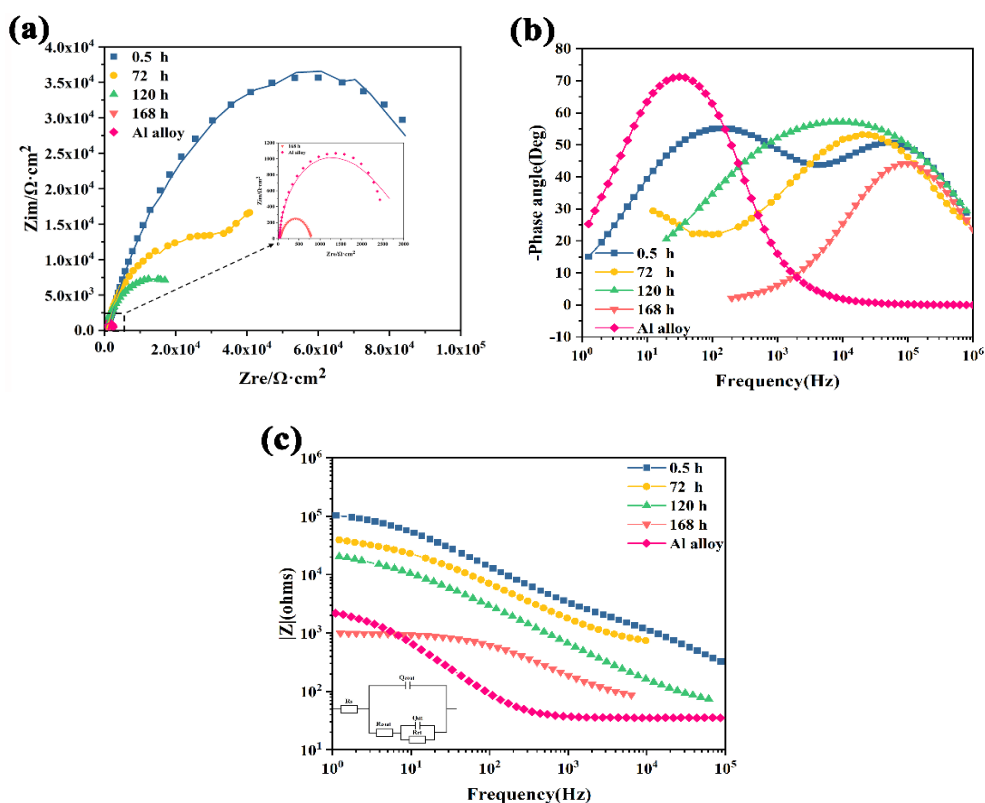

Fig. 14. (a) Nyquist; (b) Negative phase angle - frequency; (c)| Z | - frequency.

In Figure 14b, the negative phase Angle Bode diagram of the primary aluminum plate and the superhydrophobic coating shows specific characteristics. For aluminum substrates, the first time constant corresponds to the intermediate frequency region, indicating the interface between the oxide layer and the electrolyte. The second is the low frequency region, which reveals the electrochemical corrosion reaction of the aluminum substrate [65]. The experimental data show that the superhydrophobic composite coating has double constants in the middle and high frequency ranges. The superhydrophobic coating has a slightly larger intermediate frequency phase angle than the original aluminum sheet, indicating that the coating has a uniform compact nature, thus enhancing the shielding effect against corrosion [66,67]. This further proves that the superhydrophobic composite coating has good anti-corrosion performance.

From the data in Figure Figure 14c, we fitted it using the equivalent circuit to reveal the mechanism of corrosion.In an equivalent circuit, Rs represents the resistance in solution, that is, the resistance between the electrode and the coating, while Rcoat refers to the resistance of the coating. Numerally, the increase in R_{coat} indicates that the coating has better barrier properties and means that the coating has less defects[68]. Qcoat represents the constant phase Angle element of the coated sample and Qdl reflects the constant phase Angle element of the double-layer capacitor, while Rct provides an indicator to assess the permeability of the corrosive medium, and charge transfer resistance occurs through the coating hole[69]. CPE_{dl} adopts the constant phase unit, which is calculated by Brug formula as follows [70,71] :

$$C_{d1} = Q_{d1}^{\frac{1}{n}} \left(\frac{1}{R_s} + \frac{1}{R_{ct}} \right)^{\frac{n-1}{n}}$$

(2)

By using CPE values and dimensionless indicators (expressed as Q and n, respectively),the corrosion resistance of the composite coating was studied by Rct and Rcoat [72]. As can be seen from Table 3, the Rct value of the sample is as high as $1.7*10^6$ $\Omega \cdot cm^2$, while the Rct value of ordinary aluminum plate is only $3*10^2$ $\Omega \cdot cm^2$, which can also prove the excellent corrosion resistance of the sample. As the soaking time increased to 168 hours, both the Rct value and the Rcoat value of this sample decreased significantly. The reason for this phenomenon is that the protective properties of the sample coating are destroyed and the corrosive medium penetrates into the base aluminum. However, it is worth noting that the Rct value of the sample in line with the coating at this time is still much higher than that of the ordinary base aluminum. Corrosion inhibition efficiency **η** can be calculated from equation 3 [73] :

$$\eta = \left(1 - \frac{R_{ct0}}{R_{ct1}} \right) \times 100\%$$

(3)

R_{ct0} indicates the charge transfer resistance on the surface of the aluminum plate, and R_{ct1} indicates the charge transfer resistance on the surface of the sample coating.[74]The charge transfer resistance of the superhydrophobic coating is $1.7*10^6$ $\Omega \cdot cm^2$, while the aluminum sheet is $3*10^2$ $\Omega \cdot cm^2$, Therefore, the sample coating in this study can effectively reduce the amount of charge transferred between the corrosive substance and the substrate.The corrosion retarding efficiency of the sample is 99.982%, which indicates that it can prevent the corrosion of the base aluminum plate well.

In summary, the composite coating has strong corrosion resistance and long-term stability for two main reasons: first, its micro and nano structure can store air to form a long-term stable and dense air layer, which greatly reduces the direct contact between the corrosive medium and it; second, the uniform dense coating itself has a good physical corrosion shielding effect, which can effectively protect the base aluminum plate from being contacted by corrosive media for a short time.

Table 3. EIS fitting data.

sample	time h	R_s $\Omega \cdot cm^2$	R_{coat} $\Omega \cdot cm^2$	R_{ct} $\Omega \cdot cm^2$	Q_{coat} $\Omega^{-1} \cdot s^n \cdot cm^{-2}$	Q_{d1} $\Omega^{-1} \cdot s^n \cdot cm^{-2}$	n_{d1}	C_{d1} $\mu F \cdot cm^{-2}$
aluminim sheet		35.25	172	3.0×10^2	2.4×10^{-5}	—	0.95	1.19
coating	0.5	76.32	36190	1.7×10^6	5.8×10^{-8}	5.2×10^{-7}	0.78	0.7164
coating	72	75.81	34838	4.1×10^5	5.4×10^{-7}	1.7×10^{-6}	0.71	0.5876
coating	120	46.46	2297	1.1×10^5	1.9×10^{-7}	2.7×10^{-5}	0.70	0.7348
coating	168	51.22	472.7	2.4×10^3	1.0×10^{-6}	3.0×10^{-3}	0.77	0.8694

4. Conclusion

In summary, the superhydrophobic composite coating of SER /ZnO/ MWCNTs was successfully prepared by one-step spraying method, and the experiment proved that the coating had good mechanical stability and excellent corrosion resistance. Its superhydrophobic performance is significant, the contact angle is up to 167.3°, and the rolling angle is only 2.7°, which can withstand all kinds of liquids. It remains superhydrophobic after 1000 sandwear cycles and can withstand the continuous impact of 1000 g of gravel. In addition, excellent performance is maintained in harsh environments, including resistance to strong acid, strong alkali, 3.5 wt.% NaCl solution, boiling water, burning and UV light. The superhydrophobic composite coating has excellent self-cleaning and anti-fouling properties. More importantly, the electrochemical data show that its corrosion resistance is also excellent, and the anti-corrosion efficiency is as high as 99.924%.

References

[1] X.G. Li, D.W. Zhang, Z.Y. Liu, et al., Share corrosion data [J], Nature 2015, 527:442.

[2] M. Zhang, C. Li, X. Wang, et al., Corrosion Science, 2021, 190; https://doi.org/10.1016/j.corsci.2021.109685

[3] S. Akula, P. Kalaiselvi, A.K. Sahu, et al., International Journal of Hydrogen Energy, 2021, 46(34):17909-17921; https://doi.org/10.1016/j.ijhydene.2021.02.196

[4] M. Jiang, Y. Gao, S.A. Patil, et al., Power Sources, 2021, 491; https://doi.org/10.1016/j.jpowsour.2021.229595

[5] G. Gece, Corrosion Science, 2008, 50 (11):2981-2992; https://doi.org/10.1016/j.corsci.2008.08.043

[6] Y. Zhang, P. Yu, J. Wu, et al., Journal of Coatings Technology and Research, 2017; https://doi.org/10.1007/s11998-017-9978-6

[7] S.G.R. Emad, S. Morsch, T. Hashimoto, et al., Progress in Organic Coatings, 2019, 137; https://doi.org/10.1016/j.porgcoat.2019.105340

[8] R. Guo, X. Guo, H. Pei, et al., Surfaces and Interfaces, 2021, 27; https://doi.org/10.1016/j.surfin.2021.101577

[9] D. Jiang, X. Xia, J. Hou, et al., Industrial and Engineering Chemistry Research, 2018, 58(1):165-178; https://doi.org/10.1021/acs.iecr.8b04060

[10] P. Mayer, A. Dmitruk, J.W. Kaczmar, International Journal of Adhesion and Adhesives, 2021, 109; https://doi.org/10.1016/j.ijadhadh.2021.102899

[11] G. M. Wu, Z. W. Kong, J. Chen, et al., Progress in Organic Coatings, 2014, 77(2):315-321; https://doi.org/10.1016/j.porgcoat.2013.10.005

[12] H. Bahramnia, H.M. Semnani, A. Habibolahzadeh, et al., Surface and Coatings Technology, 2021, 415; https://doi.org/10.1016/j.surfcoat.2021.127121

[13] S. Zhang, J. Huang, Z. Chen, et al., Small 2017, 13; https://doi.org/10.1002/smll.201602992

[14] C.L. Xu, F. Song, X.L. Wang, et al., Chemical Engineering Journal, 2017, 313:1328-1334; https://doi.org/10.1016/j.cej.2016.11.024

[15] S. Jia, X. Lu, S. Luo, et al., Chemical Engineering Journal, 2018, 348:212-223; https://doi.org/10.1016/j.cej.2018.04.195

[16] M. Cao, X. Jin, Y. Peng, et al., Advanced Materials, 2017, 29; https://doi.org/10.1002/adma.201606869

[17] X. Tian, T. Verho, R.H.A. Ras, Science 2016, 352:142-143; https://doi.org/10.1126/science.aaf2073

[18] M. Liu, S. Wang, L. Jiang, Nature Reviews Materials 2017, 2:17036; https://doi.org/10.1038/natrevmats.2017.36

[19] S. Wang, K. Liu, X. Yao, et al., Chemical Reviews 2015, 115:8230-8293; https://doi.org/10.1021/cr400083y

[20] C. Zhang, D.A. Mcadams, J. C. Grunlan, Advanced Materials, 2016, 28:6292-6321; https://doi.org/10.1002/adma.201505555

[21] T. Sun, L. Feng, X. Gao, et al., Accounts of Chemical Research, 2005, 38:644-652; https://doi.org/10.1021/ar040224c

[22] Q. Xu, J. Li, J. Tian, et al., ACS Applied Materials Interfaces, 2014, 68976-8980; https://doi.org/10.1021/am502607e

[23] G.B. Hwang, A. Patir, K. Page, et al., Nanoscale 2017, 9:7588-7594; https://doi.org/10.1039/C7NR00950J

[24] X. Su, H. Li, X. Lai, et al., ACS Applied Materials Interfaces 2017, 9:28089-28099; https://doi.org/10.1021/acsami.7b08920

[25] W.Y. Xie, F. Wang, C. Xu, et al., Chemical Engineering Journal, 2017, 326:436-442; https://doi.org/10.1016/j.cej.2017.05.170

[26] G. Wu, J. An, X.Z. Tang, et al., Advanced Functional Materials 2014, 24:6751-6761; https://doi.org/10.1002/adfm.201401473

[27] Mohamed A M A, Abdullah A M, Younan N A., Arabian Journal of Chemistry 2015, 8(6):749-765; https://doi.org/10.1016/j.arabjc.2014.03.006

[28] L. Xie, Z. Tang, L. Jiang, et al., Surface and Coatings Technology 2015, 281:125-132; https://doi.org/10.1016/j.surfcoat.2015.09.052

[29] H. Qian, D. Xu, C. Du, et al., Journal of Materials Chemistry A, 2017, 5:2355-2364; https://doi.org/10.1039/C6TA10903A

[30] A. Caldarelli, M. Raimondo, F. Veronesi, et al., Surface and Coatings Technology 2015, 276:408-415; https://doi.org/10.1016/j.surfcoat.2015.06.037

[31] S. Li, J. Wang, Y. Li, et al., Microelectron Engineering 2015, 142: 70-76; https://doi.org/10.1016/j.mee.2015.08.009

[32] X.Q. Fan, X.J. Cui, S.J. Song, et al., Materials and Design 2022, 215:110433; https://doi.org/10.1016/j.matdes.2022.110433

[33] C. Lv, H. Wang, Z. Liu, et al., Progress in Organic Coatings 2019, 134:1-10; https://doi.org/10.1016/j.porgcoat.2019.04.042

[34] X. Guo, R. Guo, M. Fang, et al., Ceramics International 2022; https://doi.org/10.1016/j.ceramint.2022.02.293

[35] Y. Xiu, Hess D W, Wong C P., Journal of Adhesion Science and Technology., 2008, 22(15):1907-1917; https://doi.org/10.1163/156856108X320050

[36] H. Zhou, H. Wang, H. Niu, et al., Advanced Materials 2012, 24(18):2409-2412; https://doi.org/10.1002/adma.201200184

[37] F. Lin, Y. Zhong, et al., Angewandte Chemie International Edition 2004

[38] U.F. Alkaram, A.A. Mukhlis, A.H. Al-Dujaili, Journal of Hazardous Materials 2009, 169:324-332; https://doi.org/10.1016/j.jhazmat.2009.03.153

[39] J.M. Trillo, M.D. Alba, A.A. Castro, et al., Clays and Clay Minerals 1992, 27: 423-434;

https://doi.org/10.1180/claymin.1992.027.4.03

[40] S.E. Miller, G.R. Heath, R.D. Gonzalez, Clays and Clay Minerals 1982, 30:111-122; https://doi.org/10.1346/CCMN.1982.0300205

[41] J. Ou, F. Wang, W. Li, et al., Progress in Organic Coatings 2020, 146:105700; https://doi.org/10.1016/j.porgcoat.2020.105700

[42] M.R. Abukhadra, M. Mostafa, Science of the Total Environment 2019, 667:101-111; https://doi.org/10.1016/j.scitotenv.2019.02.362

[43] A.Q. Selim, E.A. Mohamed, M.K. Seliem, et al., Journal of Alloys and Compounds 2018, 762:653-667; https://doi.org/10.1016/j.jallcom.2018.05.195

[44] B.B. X, Y.W. H, B. W, Fine Chemicals 2019.

[45] X.L. Wei, N. Li, W.J. Yi, et al., Surface and Coatings Technology 2017, 325; https://doi.org/10.1016/j.surfcoat.2017.06.004

[46] W. Li, Z. Kang, Surface and Coatings Technology, 2017, 253:205- 213; https://doi.org/10.1016/j.surfcoat.2014.05.038

[47] A.M.A. Mohamed, A.M. Abdullah, N.A. Younan, Arabian Journal of Chemistry 2015, 8:749-765; https://doi.org/10.1016/j.arabjc.2014.03.006

[48] N. Wang, D. Xiong, Y. Deng, et al., ACS Applied Materials and Interfaces 2015, 7:6260-6272; https://doi.org/10.1021/acsami.5b00558

[49] C.Y. Li, P. Wang, D. Zhang, Colloid and Surfaces A: Physicochem and Engineering Aspects 2021, 624:126835; https://doi.org/10.1016/j.colsurfa.2021.126835

[50] B. Xue, C.H. Xue, S.T. Jia, ACS Applied Materials and Interfaces, 2016, 8(41):28171-28179; https://doi.org/10.1021/acsami.6b08672

[51] C.H. Xue, J.Z. Ma, Journal of Materials Chemistry A, 2013, 1:4146-4161; https://doi.org/10.1039/c2ta01073a

[52] P.C. Ma, N.A. Siddiqu, G. Marom, et al., Composites A: Applied Science Manufacturing, 2010, 41:1345-1367; https://doi.org/10.1016/j.compositesa.2010.07.003

[53] B.M. Tyson, R.K. Abu Al-Rub, A. Yazdanbakhsh, et al., Journal of Materials in Civil Engineering, 2011, 23:1028-1035; https://doi.org/10.1061/(ASCE)MT.1943-5533.0000266

[54] Y.H. Xiu, Y. Liu, D.W. Hess, et al., Nanotechnology 2010, 21:155705; https://doi.org/10.1088/0957-4484/21/15/155705

[55] T. Verho, C. Bower, P. Andrew, et al., Advanced Materials, 2011, 23:673-678; https://doi.org/10.1002/adma.201003129

[56] L. Ionov, A. Synytska, Physical Chemistry Chemical Physics, 2012, 14:10497-10502; https://doi.org/10.1039/c2cp41377a

[57] X. Kong, J. Zhang, Q. Xuan, et al., Langmuir 2018, 34(28):8294-8301; https://doi.org/10.1021/acs.langmuir.8b01423

[58] W. Liu, Q.J. Xu, J. Han, et al., Corrosion Science, 2016, 110:105-113; https://doi.org/10.1016/j.corsci.2016.04.015

[59] N. Yang, T. Yang, W. Wang, et al., Journal of Hazardous Materials, 2019, 377:142-151; https://doi.org/10.1016/j.jhazmat.2019.05.063

[60] Q.S. Zhu, E. Li, X.H. Liu, et al., Composites Part A, 2020, 130; https://doi.org/10.1016/j.compositesa.2019.105752

[61] C.W. Zhang, X.W. Li, T. Shi, et al., Rare Metal Materials and Engineering, 2018, 47(10):2980-2985; https://doi.org/10.1016/S1875-5372(18)30221-2

[62] M. Cai, X.Q. Fan, H. Yan, et al., Chemical Engineering Journal, 2021, 419:130050; https://doi.org/10.1016/j.cej.2021.130050

[63] H. Yan, M. Cai, J.C. Wang, et al., Applied Surface Science, 2021, 536:147974; https://doi.org/10.1016/j.apsusc.2020.147974

[64] T.S. Lim, H.S. Ryu, S.H. Hong, Corrosion Science, 2012, 62:104-111; https://doi.org/10.1016/j.corsci.2012.04.043

[65] Zou Y.C. Zou, Y.M. Wang, S.M. Xu, et al., Chemical Engineering Journal., 2019, 362:638-649; https://doi.org/10.1016/j.cej.2019.01.086

[66] J.R. Li, Q.T. Jiang, H.Y. Sun, et al., Corrosion Science, 2016, 111:288-301; https://doi.org/10.1016/j.corsci.2016.05.019

[67] S.Q. Wang, Y.M. Wang, J.C. Chen, et al., Journal of Magnesium and Alloys 2021; https://doi.org/10.1016/j.jma.2020.11.024

[68] Nguyen T A, Nguyen T H, Nguyen T V, et al., Surface and Coatings Technology., 2009, 204: 237-245; https://doi.org/10.1016/j.surfcoat.2009.06.048

[69] B. Han, H.Y. Wang, S.C. Yuan, et al., Progress in Organic Coatings 2020,149:105922; https://doi.org/10.1016/j.porgcoat.2020.105922

[70] J. Baux, N. Causs'e, J. Esvan, et al., Electrochim. Acta., 2018, 283:699-707; https://doi.org/10.1016/j.electacta.2018.06.189

[71] M. Faure, F. Billon, A.M. Haghiri-Gosnet, et al., Electrochim. Acta., 2018, 280:238-247; https://doi.org/10.1016/j.electacta.2018.05.116

[72] Y.W. Ye, D.W. Zhang, T. Liu, et al., Journal of Hazardous Materials 2019, 364:244-255; https://doi.org/10.1016/j.jhazmat.2018.10.040

[73] X. Liu, H.Q. He, L.K. Ouyang, et al., Journal of Alloys and Compounds 2020, 834(5):155210;https://doi.org/10.1016/j.jallcom.2020.155210

[74] M. Bharathia , K. N. Anuradhaa, M. V. Murugendrappab,Digest Journal of Nanomaterials and Biostructures,Vol.18, No.1, January-March 2023, p.343-365 ; https://doi.org/10.15251/DJNB.2023.181.343